REPORT 1334

RELATION OF TURBOJET AND RAMJET COMBUSTION EFFICIENCY TO SECOND-ORDER REACTION KINETICS AND FUNDAMENTAL FLAME SPEED

By J. Howard Childs, Thaine W. Reynolds, and Charles C. Graves

SUMMARY

Theoretical studies of the turbojet and ramjet combustion process are summarized and the resulting equations are applied to experimental data obtained from various combustor tests. The theoretical treatment assumes that one step in the over-all chain of processes which constitute jet-engine combustion is sufficiently slow to be the rate-controlling step that determines combustion efficiency. The parameter P_1T_1/V_r, based on the assumption that chemical reaction kinetics control combustion efficiency, and the parameter $P_1^{0.24}T_1/V_r^{0.76}$, derived from the assumption that the rate of flame spreading controls combustion efficiency, are evaluated for various turbojet and ramjet combustors. In these parameters P_1 is combustor-inlet static pressure, T_1 is combustor-inlet static temperature, and V_r is combustor reference velocity based on P_1, T_1, and maximum combustor cross-sectional area.

The parameter P_1T_1/V_r has been evaluated for 23 turbojet combustors; it provides an adequate correlation of the combustion efficiency of most combustors at simulated engine operating conditions but proves inadequate in some cases where combustor test conditions are varied through wide ranges. The parameter $P_1^{0.24}T_1/V_r^{0.76}$ correlates the data for two small-scale ramjet combustors but is generally unsatisfactory for correlating turbojet data. Data obtained with one combustor indicate that a shift from one rate-controlling step to another occurs as combustor pressure is increased; the parameter P_1T_1/V_r therefore best correlates the data at low pressures, while the parameter $P_1^{0.24}T_1/V_r^{0.76}$ is better at higher pressures. Thus, no single correlating parameter can be expected to be adequate for all combustors and for the entire range of operating conditions.

INTRODUCTION

One of the most serious problems encountered in the operation of jet-propelled aircraft is the reduction in combustion efficiency that occurs at high-altitude flight conditions. Experimental investigations with both turbojet and ramjet combustors have shown that combustion efficiency is adversely affected by the high velocities at which these combustors are required to operate and by the low pressures and low inlet temperatures encountered at high altitudes (ref. 1). A theory of the jet-engine combustion process is therefore needed in order to explain these effects and to indicate the design approaches that are most promising for alleviating these adverse effects. This report describes the theoretical treatment of the combustion process in turbojet and ramjet combustors and the correlation of experimental data on combustion efficiency with the theoretical equations. The NACA work in this area dates back to 1950 (refs. 2 to 7). This work was subject to security classification until 1956, at which time much of this material was presented in reference 8.

If the fuel were properly mixed with air and the fuel-air mixture were allowed adequate time in the combustor, thermodynamic equilibrium would be achieved and the combustion efficiency would be 100 percent. The occurrence of combustion efficiencies below 100 percent indicates that the conversion processes by which the chemical energy of the fuel is converted into sensible enthalpy of the exhaust products are not rapid enough to proceed to completion during the residence time allowed in high-velocity combustors.

A theoretical treatment of jet-engine combustion is difficult because of the many different conversion processes that must occur. The fuel must be vaporized, mixed with air, ignited, and oxidized to the final products of combustion. These combustion products must then be mixed with dilution air to reduce the combustor-exit temperature to the desired value. The combustion can be visualized as a competition between the conversion processes (vaporization, mixing, ignition, and oxidation) and the quenching that occurs when the reacting mixture is cooled by the dilution air and when the reacting mixture contacts the relatively cool walls of the combustor. In a ramjet combustor operating at nearly stoichiometric fuel-air ratios, dilution-air quenching ceases to be important; the efficiency is then determined by the extent to which the conversion processes proceed before the reacting mixture is swept out of the exhaust nozzle. Because of the complicated nature of the over-all process, no exact theoretical treatment is possible.

It is possible, however, to apply theoretical considerations in the analysis of the process by use of simplifying assumptions. If the rate of any one of the conversion processes is substantially less than the rates of the others, this one process will then govern the over-all rate and hence will determine the combustion efficiency. The existence of one slow conversion step in the over-all chain of processes was assumed. Combustion was then treated theoretically, assuming each of the various conversion steps to be the over-all rate-determining process. The details of the analysis are presented herein, and the results are applied to experimental data obtained with various turbojet and ramjet combustors.

ANALYSIS AND APPLICATION TO COMBUSTOR DATA

CHEMICAL REACTION KINETICS

One theoretical analysis (ref. 2) of the turbojet combustion process is based on the assumption that the chemical reaction (oxidation of the fuel) constitutes the over-all rate-determining step in the combustor. This oxidation occurs by some chain mechanism. Sometimes, however, the kinetics of chain reactions depend entirely on the kinetics of a single, slowly occurring reaction within the chain. The analysis described herein is therefore based on the kinetics of a bimolecular chemical reaction.

For the bimolecular reaction, A+B→C+D, in which A is the reactant present in smaller quantity, the reaction rate is given by the equation

$$\frac{dW}{dt}=\frac{Z\varphi\beta}{N_A} \tag{1}$$

(All symbols are defined in appendix A.) Substituting appropriate relations from the kinetic theory of gases (ref. 9) leads to

$$\frac{dX}{dt}=\frac{1}{\rho}\frac{dW}{dt}=\frac{K_3(\sigma_A+\sigma_B)^2N_B(1-X)\left(1-\frac{N_A}{N_B}X\right)Pe^{-E/RT}}{R^{1/2}T^{1/2}} \tag{2}$$

Equation (2) applies to any sample of the reacting mixture as it passes through the combustor. A detailed derivation of equation (2) is given in appendix B and in reference 2.

At this point in the analysis, two somewhat different approaches are taken. These are treated as the nonhomogeneous reactor and the homogeneous reactor, respectively.

Nonhomogeneous reactor.—Figures 1 and 2 show values of fuel-air mixture composition within the burning zone of a typical turbojet combustor; these data were obtained by a water-cooled sampling probe. The vapor fuel-air ratio decreases progressively along the length of the combustor, and marked variations in composition occur over the combustor cross section. The data of figures 1 and 2 indicate that homogeneity is not approached. The rate of mixing of fuel and air may nevertheless be quite rapid. Rapid fuel-air mixing is assumed in this portion of the paper; possible effects of slow mixing rates are treated in the section on Other Conversion Processes.

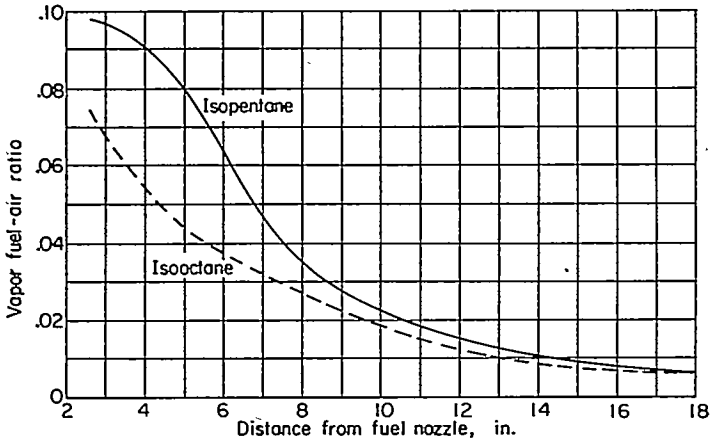

FIGURE 1.—Variation of vapor fuel-air ratio with distance from fuel nozzle in typical tubular turbojet combustor. Simulated high altitude; over-all fuel-air ratio, 0.007.

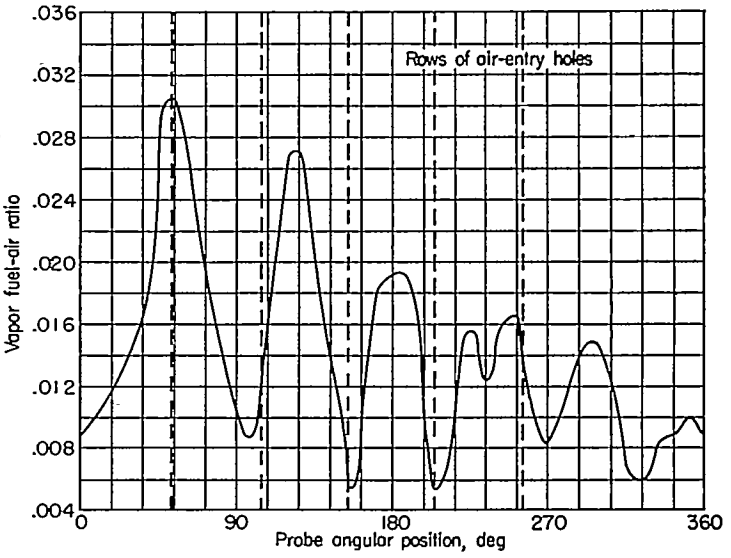

FIGURE 2.—Variation of fuel-air ratio with angular position of sampling probe 12½ inches downstream of fuel nozzle in a typical tubular turbojet combustor. Fuel, isooctane; over-all fuel-air ratio, 0.014.

The major assumptions in this analysis may be summarized as follows:

(1) Reaction occurs in local zones of stoichiometric fuel-air ratio that exist at the interface between the fuel-rich and air-rich regions.

(2) The mixing process whereby fuel and air are introduced to the reaction zone is sufficiently rapid that the chemical reaction rate controls the over-all process.

(3) The temperature in the reaction zone is constant along the combustor at a value close to the stoichiometric flame temperature.

(4) The mean concentration of each reactant in the reaction zone varies along the combustor and is equal to the initial concentration minus the fraction X that has already reacted at any position in the combustor.

The foregoing assumptions do not necessarily constitute those characterizing the simplest or most plausible physical model of the combustion process. Rather, they constitute the assumptions necessary to arrive at a final equation that fits the experimental data.

At the outlet of the reaction zone, X is equal to η_b, because the particular reaction under consideration is the one governing the over-all process. Thus,

$$X=\eta_b \text{ when } l=L \text{ and } t=L/V_a, \tag{3}$$

Integrating equation (2) with the assumption that the temperature in the zone where the reaction A+B→C+D occurs is substantially constant and substituting from equation (3) give

$$\ln\frac{1-\frac{N_A}{N_B}\eta_b}{1-\eta_b}+K_2=\frac{K_3(\sigma_A+\sigma_B)^2(N_B-N_A)LPe^{-E/RT}}{V_aR^{1/2}T^{1/2}} \tag{4}$$

The foregoing equation is expressed in terms of the values

of P, T, and V_{av} in the reaction zone. In experimental investigations, these variables are not measured; the values of the combustor-inlet variables P_t, T_t, and V_r are usually determined. The values of P, T, and V_{av} must therefore be expressed in terms of combustor-inlet conditions. When appropriate approximations and substitutions are made (appendix C),

$$\ln\frac{1-\frac{N_A}{N_B}\eta_b}{1-\eta_b}+K_2=\frac{K_3(\sigma_A+\sigma_B)^2(N_B-N_A)e^{-E/RT}}{R^{1/2}T^{3/2}}\times \left[\frac{L\left(1-\frac{\Delta P}{P_t}\right)^2}{\frac{\sum_p A_h C_d}{\sum_t A_h C_d}\left(\frac{A_r}{A_a}\right)}\right]\frac{P_t T_t}{V_r} \tag{5}$$

On the right side of equation (5) the terms are grouped into (1) those dependent upon fuel type and fuel-air ratio, (2) those dependent upon combustor design, and (3) those dependent only upon the operating conditions.

For a given combustor operating with a given fuel at a fixed fuel-air ratio and with negligible pressure drop assumed across the combustor, equation (5) becomes

$$\ln\frac{1-\frac{N_A}{N_B}\eta_b}{1-\eta_b}+K_2=K_4\frac{P_t T_t}{V_r} \tag{6}$$

The same relation can be expressed as

$$\eta_b=f\left(\frac{P_t T_t}{V_r}\right)=f'\left(\frac{P_t^2}{w_a}\right) \tag{7}$$

Figures 3 and 4 show experimental data obtained with an annular turbojet combustor (combustor 1) plotted in accordance with equations (6) and (7), respectively. A straight-line data correlation is obtained in figure 3, as predicted by equation (6). Data for a range of fuel-air ratios are included in both figures 3 and 4. The theoretical equations apply only for a fixed fuel-air ratio; however, for this particular combustor the efficiency did not vary appreciably with change in fuel-air ratio in the range investigated.

The parameter $P_t T_t/V_r$ has been used extensively at the NACA Lewis laboratory to correlate the combustion efficiency of turbojet combustors. Combustion efficiencies obtained with 23 experimental and production-model turbojet combustors have been plotted against $P_t T_t/V_r$. The data correlations for 14 turbojet combustors are presented in reference 2; the other correlations are unpublished. For most combustors the correlation is good; but for others the data scatter is great and $P_t T_t/V_r$ cannot be used to predict combustion efficiency. For combustors in which combustion efficiency varies appreciably with fuel-air ratio, a satisfactory correlation can be obtained only by using a different correlation curve for each narrow range of fuel-air ratio. Illustrative examples of the correlations obtained for two other turbojet combustors are shown in figure 5. The data for combustor 3 (fig. 5(b)) represent the poorest correlation obtained in the many applications of the $P_t T_t/V_r$ parameter.

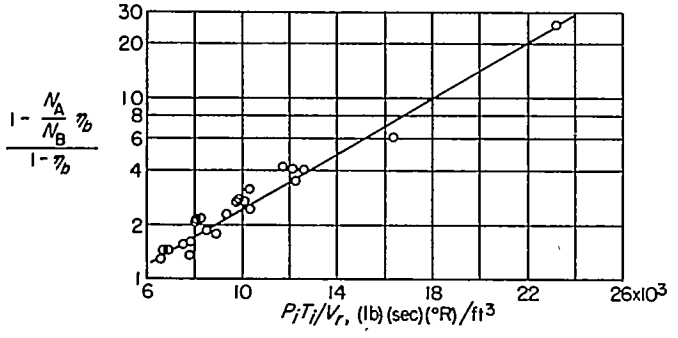

FIGURE 3.—Experimental data obtained with combustor 1 plotted in accordance with equation (6). Fuel, gasoline; variable fuel-air ratio.

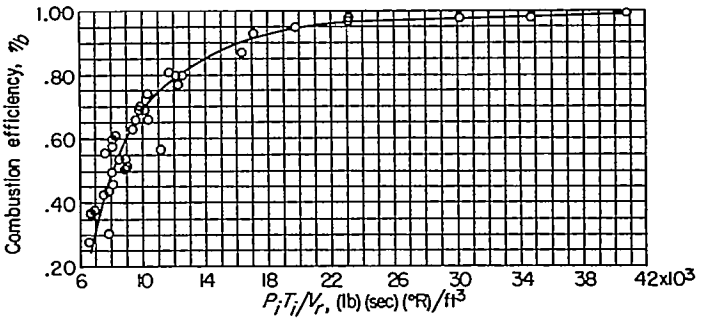

FIGURE 4.—Experimental data obtained with combustor 1 plotted in accordance with equation (7). Fuel, gasoline; variable fuel-air ratio.

Homogeneous reactor.—When the mixing in the combustor is assumed to be sufficiently rapid to produce a homogeneous mixture throughout the combustor volume,

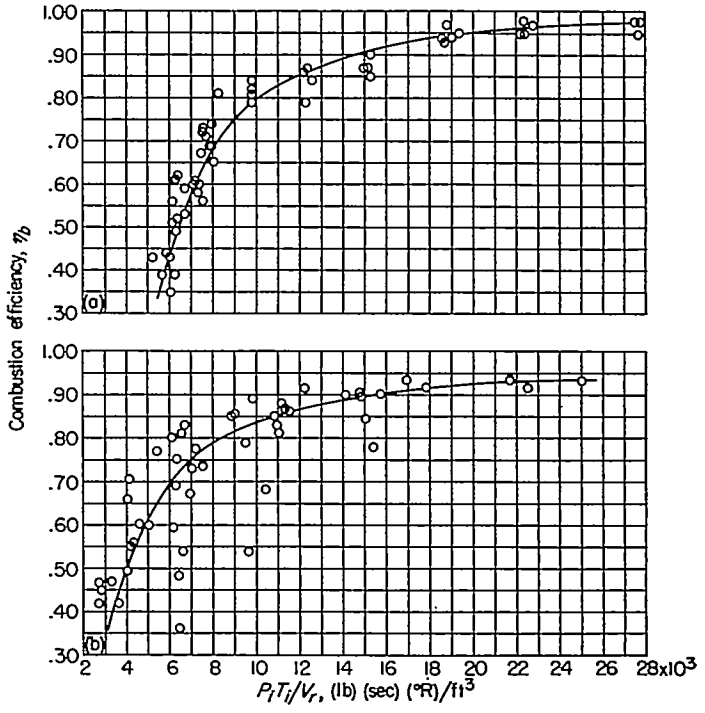

(a) Combustor 2.
(b) Combustor 3.

FIGURE 5.—Experimental data for turbojet combustors plotted in accordance with equation (7). Fuel, AN-F-28.

for given operating conditions the value of X is constant over the combustor reaction zone, and it is no longer necessary to integrate the equation as in the preceding analytical approach. A homogeneous reaction zone was also assumed in reference 10 in analyzing the combustion process in a can-type combustor having a premixed fuel-air feed and in reference 11 in analyzing flames in the wake of bluff bodies.

For this condition $T \cong T_t + \Delta T_s \eta_b$,

$$\eta_b = \left(\frac{dW}{dt}\right)\left(\frac{1}{\rho}\right) t = \frac{K_3(\sigma_A+\sigma_B)^2 N_B (1-\eta_b)\left(1-\frac{N_A}{N_B}\eta_b\right) P L e^{-E/R(T_t+\Delta T_s \eta_b)}}{R^{1/2}(T_t+\Delta T_s\eta_b)^{1/2} V_a} \tag{8}$$

Rearranging terms yields

$$\frac{\eta_b (T_t+\Delta T_s\eta_b)^{3/2} e^{\frac{E}{R(T_t+\Delta T_s\eta_b)}}}{(1-\eta_b)\left(1-\frac{N_A}{N_B}\eta_b\right)} = \frac{K_3(\sigma_A+\sigma_B)^2 N_B}{R^{1/2}}\left[\frac{L\left(1-\frac{\Delta P}{P_t}\right)^2}{\frac{\sum_p A_h C_d}{\sum_t A_h C_d}\left(\frac{A_r}{A_a}\right)}\right]\frac{P_t T_t}{V_r} \tag{9}$$

Here again the terms on the right side of the equation are grouped into (1) those dependent upon fuel type and fuel-air ratio, (2) those dependent upon combustor design, and (3) those dependent only upon operating conditions. For a given combustor, a given fuel, and a single fuel-air ratio, equation (9) becomes

$$\frac{\eta_b (T_t+\Delta T_s\eta_b)^{3/2} e^{\frac{E}{R(T_t+\Delta T_s\eta_b)}}}{(1-\eta_b)\left(1-\frac{N_A}{N_B}\eta_b\right)} = K_5 \frac{P_t T_t}{V_r} \tag{10}$$

The data for combustor 1 were plotted in accordance with equation (10). The fact that the predicted straight-line relation was not obtained indicates that the assumption of nonhomogeneity (eq. (6)) better fits the experimental data for this particular combustor than the assumption of homogeneity (eq. (10)). This is as expected, since figures 1 and 2 indicate that a condition of homogeneity is not approached within a typical turbojet combustor. For combustors having higher rates of mixing in the combustion space than those existing in most turbojet and ramjet combustors, equation (10) may afford a better correlation of the data. Equation (10) can also be expressed as

$$\eta_b = f\left(\frac{P_t T_t}{V_r}, T_t\right) \tag{11}$$

and, since T_t is small compared with ΔT_s, for a reasonable correlation of engineering data for which T_t does not vary widely, it might be assumed that

$$\eta_b = f\left(\frac{P_t T_t}{V_r}\right) = f'\left(\frac{P_t^2}{w_a}\right) \tag{7}$$

This equation is the same as that obtained for the nonhomogeneous reactor.

FLAME SPREADING

Since flame speed is one of the fundamental combustion properties that can readily fit into a physical picture of the combustion process, a simplified analysis was also made assuming combustion efficiency to be controlled by the rate of flame spreading. The combustion process was visualized as the burning of fuel-air globules of random size and shape, which are surrounded by a flame surface and which are consumed as they pass through the combustor. The flame surface advances into the adjacent unburned mixture at a rate determined by the physical conditions of the mixture. The effect of turbulence on the rate of flame spreading is considered solely in terms of its effect on the flame surface area.

The combustion efficiency may be expressed as follows:

$$\eta_b = \frac{\rho_u S U_L}{\rho_u A_r V_r} \tag{12}$$

The numerator represents the mass of combustible consumed by the flame per unit time; the denominator represents the mass flow through the combustor per unit time. Hence, the ratio of these two quantities must equal the combustion efficiency.

Bunsen-burner experiments (refs. 12 to 14) have shown that

$$\frac{U_T}{U_L} \propto Re^{0.24} P_t^{0.3} \propto S \tag{13}$$

if it is assumed that the effect of turbulence on flame speed is due to flame wrinkling (increase in S). For isooctane-air mixtures (ref. 15),

$$U_L \propto T^{1.4} \tag{14}$$

The effect of variations in ambient pressure on the laminar flame speeds of hydrocarbon fuel-air mixtures has not been definitely established. The effect is small and appears to vary with fuel type. In general, the relation between the flame speed and pressure can be expressed in the form

$$U_L \propto P_t^q \tag{15}$$

for hydrocarbon fuel-air mixtures. Here q generally has a value ranging from $-\frac{1}{8}$ to approximately 0. Reference 16 concludes that the flame speeds of hydrocarbon fuel-air mixtures should be independent of pressure if the tube diameter is large enough to prevent surface effects from becoming important. In reference 17, the flame speed of vaporized isooctane-air mixtures was found to be inversely proportional to the cube root of the ambient pressure. Reference 18 (p. 177) shows that the exponent q in equation (15) depends on the flame speed of the fuel. For fuels having flame speeds of the order of that of isooctane, the value of q is zero. For propane-air mixtures, reference 19 gives $q=-0.3$ and reference 20 gives $q=-0.19$. A value of $q=-0.3$ was selected for use in this derivation, since when this value is substituted into equation (13) the turbulent

flame speed is independent of pressure, a fact which has been demonstrated for propane-air mixtures (ref. 13).

With these substitutions, equation (12) becomes

$$\eta_b = K_6 \frac{Re^{0.24} P_i^{0.3} T_i^{1.4}}{P_i^{0.3} V_r} \tag{16}$$

Substituting $Re = K_2 P_i V_r / T_i^{1.7}$ into equation (16) gives

$$\eta_b = f\left(\frac{P_i^{0.24} T_i}{V_r^{0.76}}\right) \tag{17}$$

The parameter derived from the assumption that flame spreading governs the over-all combustion rate did not correlate the data for combustor 1, as evidenced by the scatter of data points in figure 6. However, most of the data points do lie close to a common curve. Thus, the flame-speed parameter might possibly correlate data over a part of the combustor operating range, and a more critical evaluation of this parameter appears warranted.

Data obtained with two 5-inch-diameter ramjet combustors (ref. 6) are plotted in accordance with equation (17) in figure 7. One of these combustors (combustor 4) employed a V-gutter flameholder and the other (combustor 5) a conical flameholder. In both combustors the fuel was injected well upstream of the flameholder so that a homogeneous fuel-air mixture entered the combustor. The flame-spreading parameter of equation (17) gave a reasonably good correlation of the ramjet combustor data. Data for two fuels, gasoline and isopentane, fall on the same curve; this is not surprising, since the fundamental flame speeds of these fuels do not differ appreciably.

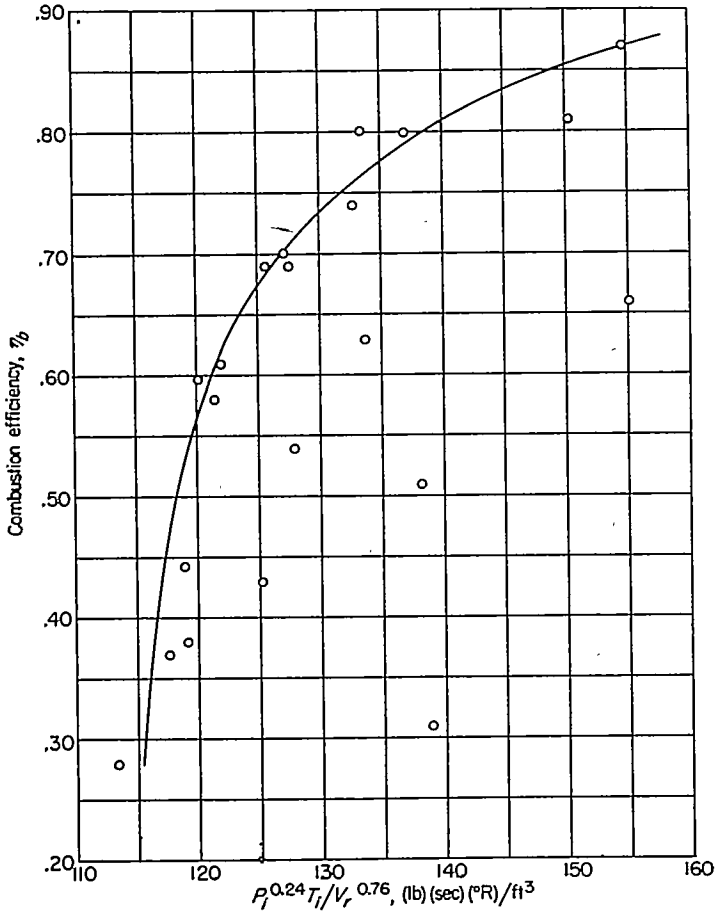

FIGURE 6.—Experimental data obtained with combustor 1 plotted in accordance with equation (17). Fuel, gasoline; variable fuel-air ratio.

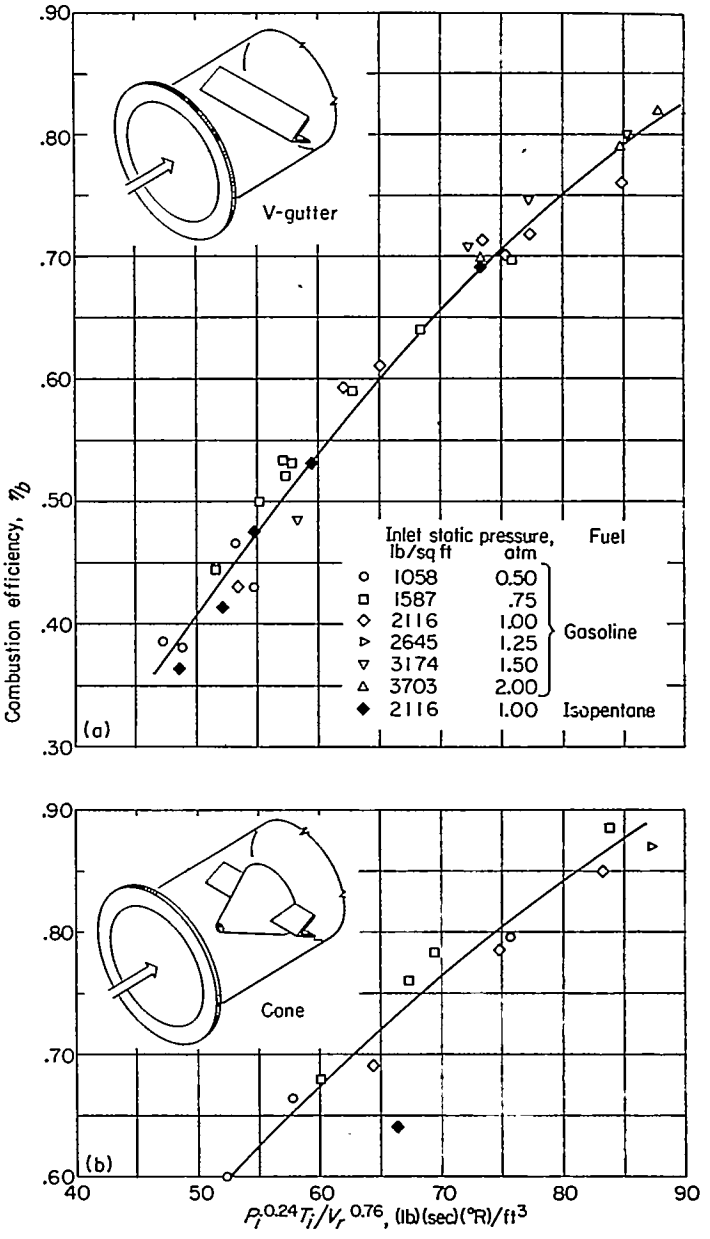

(a) Combustor 4. (b) Combustor 5.

FIGURE 7.—Experimental data obtained with 5-inch-diameter ramjet combustors plotted in accordance with equation (17). Fuels, isopentane and gasoline.

For variations in fuel type giving sizable variations in U_L, equation (17) becomes

$$\eta_b = f\left(\frac{P_i^{0.24} T_i}{V_r^{0.76}} \frac{U_L}{U_{L,r}}\right) \tag{18}$$

where $U_{L,r}$ is the flame speed of a reference fuel. Gasoline was selected as the reference fuel, giving $U_{L,r} = 1.4$ feet per second. Data for combustor 4 operating with 16 different fuels (ref. 7) are plotted in accordance with equation (18) in figure 8. Only the data for carbon disulfide deviate badly from the common curve.

OTHER CONVERSION PROCESSES

In addition to those already discussed, analyses of the jet-engine combustion process were also made with the assumption that (1) fuel vaporization, (2) fuel-air turbulent mixing, and (3) fuel-droplet burning (governed by heat transfer into the droplet) were the rate-determining steps in the over-all combustion process. With each of these three analyses, the predicted effects on combustion efficiency of operating variables such as combustor-inlet pressure, combustor velocity, and combustor-inlet temperature differed markedly from the effects observed experimentally; that is, the equations relating P_t, T_t, and V_r derived in these analyses differed greatly from equation (7) and gave no correlation of experimental data. The results of one of these analyses have been published in reference 21, which presents the change in burning rate of single fuel droplets resulting from a change in oxygen concentration of the ambient atmosphere. This change in droplet burning rate is much less than that required for this phenomenon to account for the observed change in combustion efficiency with change in inlet oxygen concentration in a typical turbojet combustor.

Since none of these three analyses provided agreement between theoretical and experimental data, the tentative conclusion may be drawn that neither fuel vaporization, fuel-air mixing, nor fuel-droplet burning alone constitutes the rate-determining, slowest step in the combustion process. The analyses were, however, based on certain simplifying assumptions similar to the assumptions included in the analyses of the chemical reaction kinetics and flame spreading, which were previously discussed. Therefore, the possibility cannot be overlooked that different assumptions in these analyses might result in closer agreement between theory and experimental data.

EXPERIMENTAL VERIFICATION OF THEORY

VARIATION OF OXYGEN CONCENTRATION

In order to test the applicability of the equations previously derived, a number of special experiments were conducted. Investigations of mixtures of vapor fuel, oxygen, and nitrogen show marked effects of oxygen concentration on such fundamental combustion properties as minimum spark-ignition energy, quenching distance, and flame speed (refs. 15 and 22). Oxygen concentration appreciably affects equilibrium flame temperature at stoichiometric or richer fuel-air ratios and also affects the concentration of the chemical species involved in the combustion; oxygen concentration is therefore a means of varying the kinetics of the chemical reactions.

In combustor tests, variations in oxygen concentrations should affect the rate of combustion without appreciably changing such factors as inlet velocity, turbulent mixing associated with inlet conditions, and fuel-spray characteristics. This experimental device should simplify interpretation and application of the test data. Accordingly, an investigation was conducted (refs. 3 and 4) to determine the effect of inlet oxygen concentration on the combustion efficiency of a tubular turbojet combustor (combustor 6). Combustion-efficiency data were obtained for the combustor operating both with liquid isooctane and with gaseous propane over a range of combustor-inlet pressures and oxygen concentrations. The combustor-inlet temperature and the oxygen-nitrogen-mixture mass-flow rate were held constant in these tests.

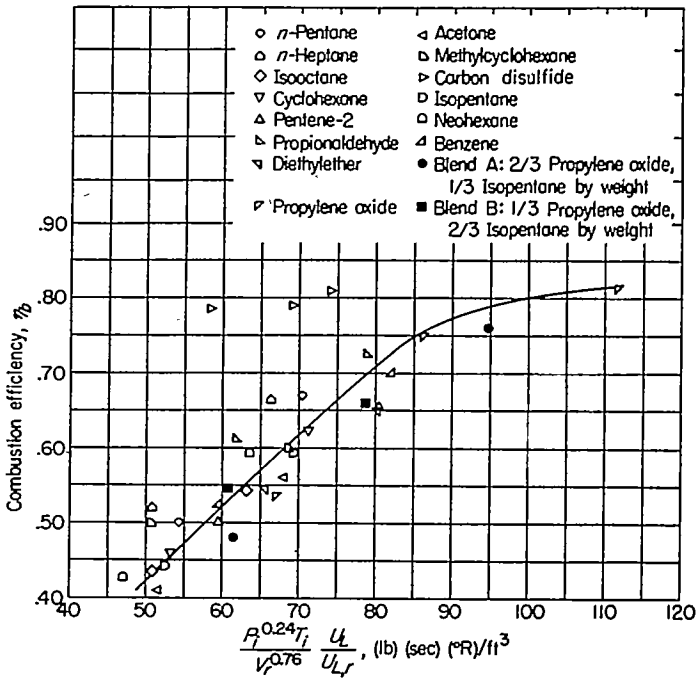

FIGURE 8.—Combustion-efficiency data obtained for V-gutter flameholder in 5-inch-diameter ramjet combustor for 14 pure fuels and two blends (ref. 7), plotted in accordance with equation (18).

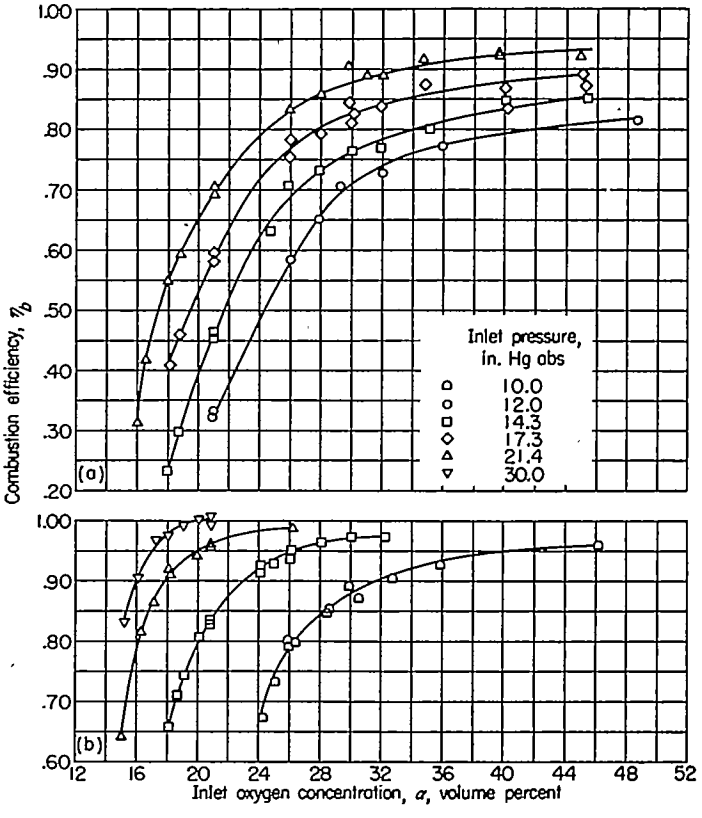

(a) Liquid isooctane fuel. (b) Gaseous propane fuel.

FIGURE 9.—Sample of experimental data obtained with combustor 6 and varying inlet oxygen concentration. Fuel-air ratio, 0.012; inlet-air temperature, 40° F.

A typical set of data obtained for the combustor operating with liquid isooctane and gaseous propane is shown in figure 9. There are pronounced changes in combustion efficiency with variation in both combustor-inlet pressure and oxygen concentration. Data of this type were treated in terms of both the second-order reaction and the flame-speed equations previously derived.

In the application of equation (5) to the oxygen-enrichment data, the burning-zone temperature was arbitrarily taken as the stoichiometric adiabatic equilibrium temperature, and the concentration of one of the reactants was assumed to be proportional to the oxygen concentration α of the combustor-inlet oxygen-nitrogen mixture. Under these conditions, the ratio N_A/N_B can be assumed constant; and, for a given combustor, fuel, and fuel-oxygen-nitrogen mixture ratio, equation (5) can be expressed in the form

$$\eta_b = f\left[\frac{\alpha P_i T_i}{V_r}\left(\frac{e^{-\frac{E}{RT_{eq}}}}{T_{eq}^{3/2}}\right)\right] \tag{19}$$

Here T_{eq} is the stoichiometric adiabatic equilibrium temperature, which is a function of oxygen concentration.

The application of equation (19) to the data of figure 9(a) is shown in figure 10. The equilibrium temperatures at the various combustor-inlet pressures and oxygen concentrations were computed by the methods and charts of reference 23. For the combustor data obtained with liquid isooctane, an apparent energy of activation E of approximately 37,000 calories per gram mole satisfactorily correlated the data. (In fig. 10 the constant 33,500 is equivalent to E/R; if this value is multiplied by $R=1.987$ and divided by 1.8 to convert the units, the value of approximately 37,000 is obtained for E.) This value of E is in reasonable agreement with the apparent energy of activation of 32,000 calories per gram mole obtained from adiabatic compression data for isooctane-air mixtures (ref. 24). for flame-speed data of isooctane-oxygen-nitrogen mixtures, reference 15 found that a value of 40,000 gave closer agreement between experimental and predicted flame speeds than did 32,000 calories per gram mole. The effect of fuel-air ratio on the form of the correlation curves is shown in figure 11, where faired curves are drawn through the correlated data for the various fuel-flow rates.

The data obtained for combustor 6 operating with gaseous propane were correlated in a similar fashion. Figure 12 shows the correlation in terms of equation (19) for the combustor operating at a fuel-air ratio of 0.012. The value of apparent energy of activation E required for best correlation varied from approximately 27,000 in the low combustion-efficiency range to approximately 33,000 calories per gram mole in the high combustion-efficiency range. Since the scatter of the correlation in the low combustion-efficiency range was quite sensitive to the value E, a value of E of 28,000 calories per gram mole was used for figure 12. The accuracy of measurements of combustor operating variables was not good enough to warrant the determination of a more exact value of E between 27,000 and 33,000 calories per gram mole. This range of values of E is in approximate agreement with that cited for propane in the literature. In reference 22, a value of 38,000 calories per gram mole is given. However, unpublished observations in the application of the Semenov theory to flame-speed data of propane-oxygen-nitrogen mixtures indicate that a value of 34,000 calories per gram mole resulted in better agreement between experimental and predicted values.

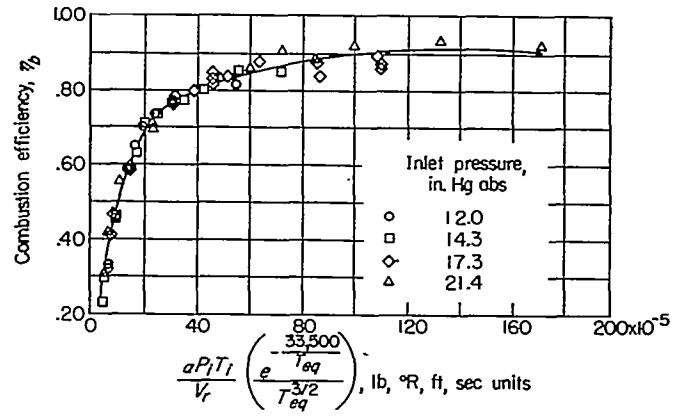

FIGURE 10.—Experimental data obtained with combustor 6 (fig. 9(a)), plotted in accordance with equation (19). Fuel, isooctane; fuel-air ratio, 0.012; inlet-air temperature, 40° F.

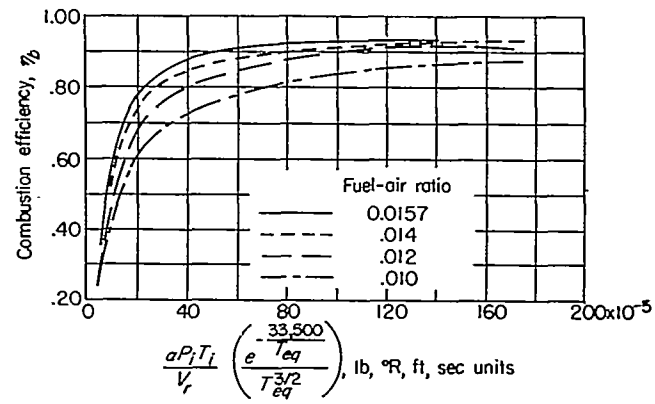

FIGURE 11.—Effect of fuel-air ratio on correlation of data for combustor 6. Fuel, isooctane; inlet-air temperature, 40° F.

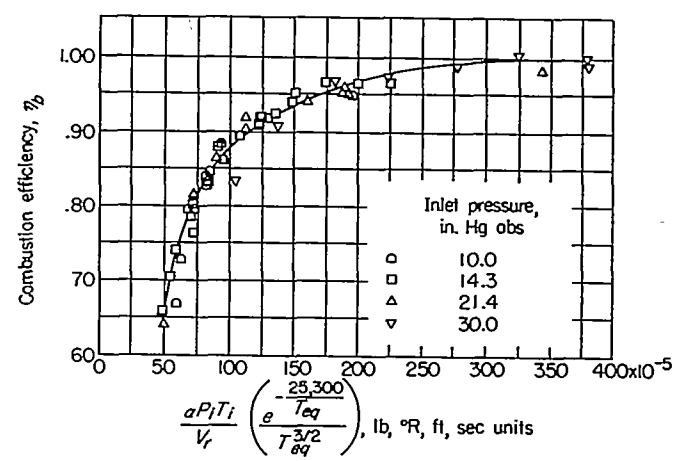

FIGURE 12.—Experimental data obtained with combustor 6 (fig. 9(b)), plotted in accordance with equation (19). Fuel, propane; fuel-air ratio, 0.012; inlet-air temperature, 40° F.

For combustor data obtained at constant inlet temperature and including variations in the inlet oxygen-nitrogen mixture composition, the flame-spreading equation (eq. (12)) reduces to

$$\eta_b = f\left(\frac{P_i^{0.24} U_L}{V_r^{0.76}}\right) \tag{20}$$

Here the small change in Reynolds number resulting from the change in viscosity of the inlet mixture with oxygen concentration is neglected.

In reference 15, the laminar flame speeds of isooctane-oxygen-nitrogen mixtures at atmospheric pressure and various equivalence ratios were determined over a range of initial mixture temperatures and oxygen concentrations. The maximum flame speed U_L was found to be directly proportional to the term $\alpha-12$. Similar data were obtained for propane-oxygen-nitrogen mixtures (unpublished NACA data). For oxygen concentrations of 30 percent by volume and below, the flame speed was found to be proportional to the term $\alpha-11.5$. The constant of 11.5, which represents the extrapolated value of α for U_L of zero, is in agreement with the value of 11.6 cited in reference 25 for the concentration limit of flammability. Substituting these correlation terms for the effect of oxygen concentration on maximum flame speed in equation (20) gives the following flame-speed equations for constant combustor-inlet temperature:

For isooctane:

$$\eta_b = f\left[\frac{P_i^{0.24}(\alpha-12)}{V_r^{0.76}}\right] \tag{21}$$

For propane:

$$\eta_b = f\left[\frac{P_i^{0.24}(\alpha-11.5)}{V_r^{0.76}}\right] \tag{22}$$

In these equations the laminar flame speeds of both isooctane and propane are assumed to have the same pressure dependence. The combustion-efficiency data are correlated for isooctane and propane in combustor 6 in terms of the preceding flame-speed parameters in figures 13 and 14. The isooctane data correlate well; however, the propane data obtained at the lower combustor pressures fall well below the data for higher pressures.

The reaction-kinetics parameter of equation (19) and the flame-spreading parameter of equation (21) both correlate the isooctane data obtained with combustor 6. In these data only the combustor-inlet pressure and the inlet oxygen concentration were varied. Evidently the relative effects of P_i and α are the same in these equations for the range of values investigated in the tests with combustor 6. No clear-cut explanation is available for the failure of equation (22) to correlate the data obtained with combustor 6 operating with propane fuel. However, the combustor was operated at lower pressure with propane fuel than with isooctane, and the low-pressure data fall farthest from the correlation curve.

INDEPENDENT VARIATION OF COMBUSTOR-INLET PRESSURE AND AIRFLOW RATE OVER WIDE RANGES

The assumption that chemical reaction kinetics govern the over-all combustion rates led to the prediction that combustion efficiency could be correlated as a function of the parameter $P_i T_i / V_r$, and this parameter is equal to a dimensional constant times the parameter P_i^2/w_a. The assumption that the rate of flame spreading governs the over-all combustion rate led to the prediction that combustion efficiency should correlate as a function of the parameter $P_i^{0.24} T_i / V_r^{0.76}$. This parameter is equivalent to a dimensional constant times $P_i^{1.0} T_i^{0.24} / w_a^{0.76}$. The reaction-kinetics analysis therefore yields a ratio of exponents of the pressure and airflow-rate terms of 2, while the flame-speed analysis yields

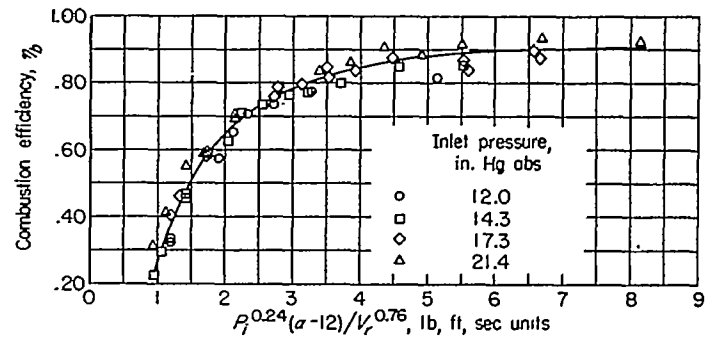

FIGURE 13.—Experimental data obtained with combustor 6 (fig. 9(a)), plotted in accordance with equation (21). Fuel, isooctane; fuel-air ratio, 0.012; inlet-air temperature, 40° F.

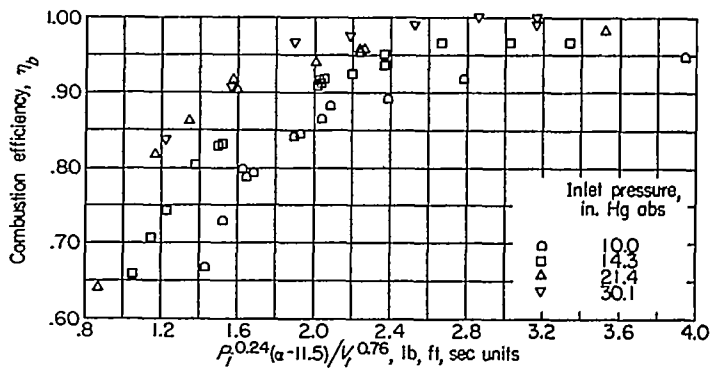

FIGURE 14.—Experimental data obtained with combustor 6 (fig. 9(b)), plotted in accordance with equation (22). Fuel, propane; fuel-air ratio, 0.012; inlet-air temperature, 40° F.

a ratio of these same exponents of 1.32. Obviously both of these parameters cannot adequately correlate the combustion-efficiency data where the combustor pressure and combustor airflow rate are varied through wide ranges. However, both of these parameters do provide a satisfactory correlation of the isooctane data for combustor 6 (figs. 10 and 13). This is possible only because these data were obtained for combustor operation at a single value of airflow rate.

In order to determine conclusively whether the ratio of exponents on the pressure and airflow-rate terms should be 2, 1.32, or perhaps neither of these values, it was necessary to conduct a series of combustor tests in which the pressure

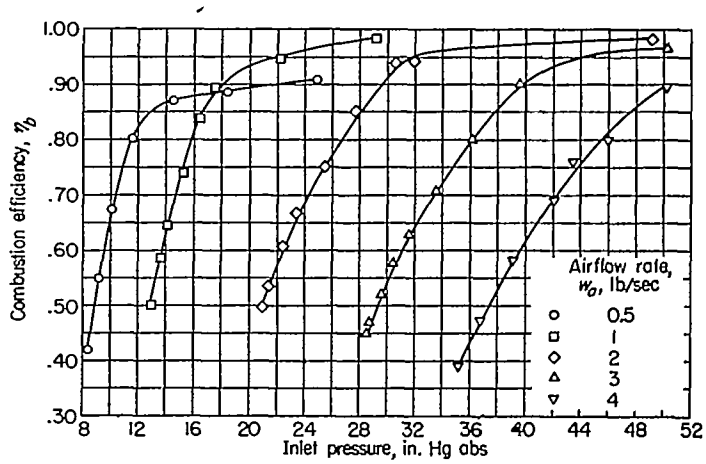

FIGURE 15.—Sample of data obtained with combustor 6 for wide variation in inlet pressure and airflow rate. Fuel, propane; fuel-air ratio, 0.012; inlet-air temperature, 80° F.

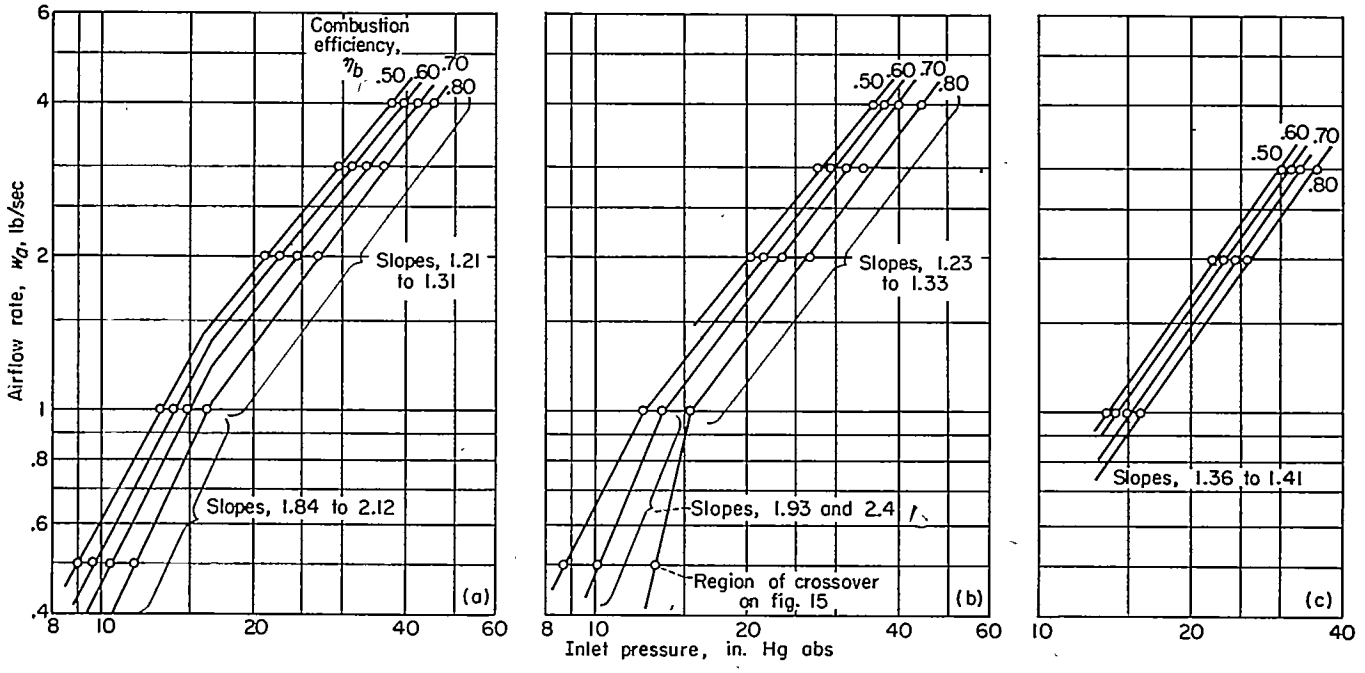

(a) Fuel-air ratio, 0.012. (b) Fuel-air ratio, 0.008. (c) Fuel-air ratio, 0.016.

FIGURE 16.—Cross plot from faired curves of figure 15 to determine relative effects of inlet pressure and airflow rate on combustion efficiency.

and airflow rate were independently varied over wide ranges. Such an investigation was conducted in turbojet combustor 6 using gaseous propane fuel and a single-orifice fuel injector (ref. 5). A sample of the experimental data is shown in figure 15, where combustion efficiency is plotted against combustor-inlet pressure with parametric lines of airflow rate. The data of figure 15 are for a fuel-air ratio of 0.012; similar data were obtained for fuel-air ratios of 0.008 and 0.016.

The data of figure 15 are cross-plotted in figure 16(a), where combustor airflow rate is plotted against combustor pressure with parametric lines of combustion efficiency. The slope of the lines in figure 16(a) indicates the ratio of exponents on the pressure and airflow rate terms of the correlating parameter that best fits the experimental data. A transition is evident in the vicinity of a combustor pressure of 15 inches of mercury. At the very low values of combustor pressure and airflow rate, the slope of the curves is approximately 2, which agrees with the slope predicted by the parameter $P_t T_t / V_r$. At high values of combustor airflow rate and pressure, however, the slope of the curves is of the order of 1.3, which agrees with the value predicted by the parameter $P_t^{0.24} T_t / V_r^{0.76}$.

Similar plots of the data obtained at fuel-air ratios of 0.008 and 0.016 are shown in figures 16(b) and (c), respectively. The data of figure 16(b) again indicate a transition in the curves, the slope being approximately 2 at low values of pressure and airflow rate and approximately 1.3 at the higher values. The data for a fuel-air ratio of 0.016 do not extend to pressures below about 14 inches of mercury; hence the transition in slope of the curves was not obtained in figure 16(c).

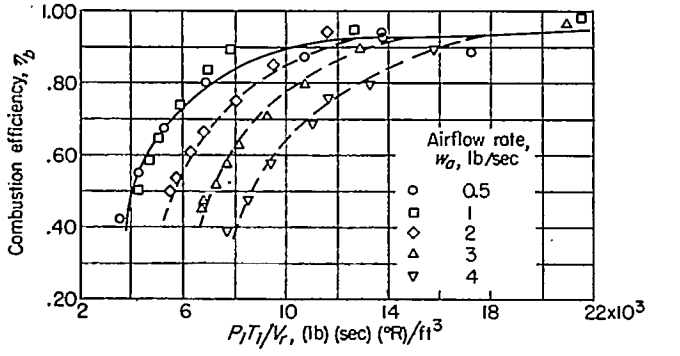

FIGURE 17.—Experimental data obtained with combustor 6 (fig. 15), plotted in accordance with equation (7). Fuel, propane; fuel-air ratio, 0.012; inlet-air temperature, 80° F.

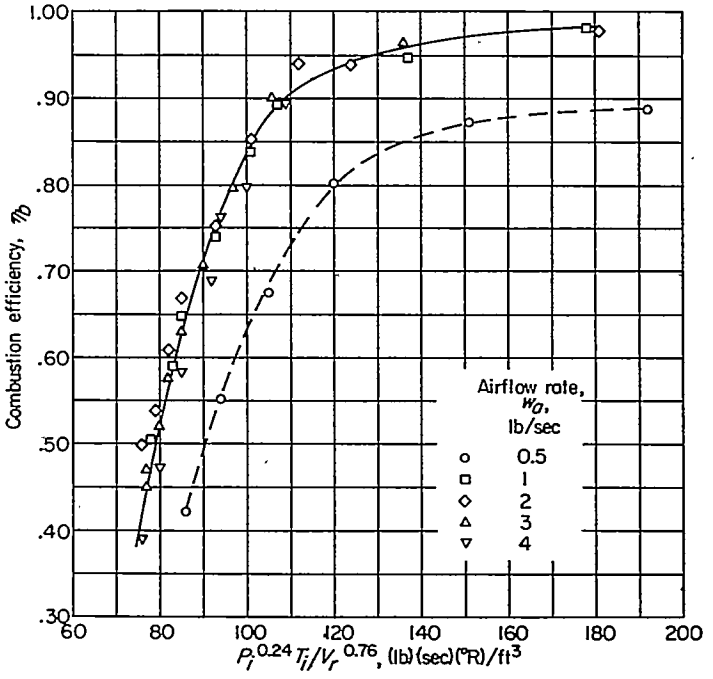

FIGURE 18.—Experimental data obtained with combustor 6 plotted in accordance with equation (17). Fuel, propane; fuel-air ratio, 0.012; inlet-air temperature, 80° F.

The data of figure 16 indicate that, for this particular combustor, the parameter $P_t T_t/V_r$ will correlate data obtained at the low values of pressure and airflow rate, while the parameter $P_t^{0.24} T_t/V_r^{0.76}$ will correlate the data obtained at higher values of pressure and airflow rate. Neither parameter, however, adequately correlates data obtained over the entire range of pressures and airflow rates. This prediction is verified by the data of figures 17 and 18, where the data of figure 15 are plotted as a function of the parameters $P_t T_t/V_r$ and $P_t^{0.24} T_t/V_r^{0.76}$, respectively.

DISCUSSION

Although the data of figure 16 are meager and therefore insufficient to warrant definite conclusions regarding the combustion mechanism, there is indication that a shift from one rate-controlling process to some other rate-controlling process occurs as combustor operating conditions are varied through wide ranges. The data of figure 16, together with the analyses presented earlier in this paper, indicate that at very low values of pressure in the combustor the chemical reaction kinetics are the rate-controlling process. At higher pressures, however, the rate of flame spreading appears to be the rate-determining process. This trend of events is at least in qualitative accord with expectations, for the chemical reaction kinetics are a function of the square of combustor pressure and would therefore be expected to be very slow at low-pressure conditions and increase rapidly with increase in pressure until some pressure is reached above which kinetics no longer constitute the slowest step in the over-all chain of processes. More extensive investigations with other combustors would be required, however, before any definite conclusions could be made in this regard.

Other investigators (e. g., refs. 26 and 27) have obtained correlating parameters different from those presented herein. In their correlating parameters the ratio of exponents on the pressure and airflow-rate terms lies between the values of 1.3 and 2 obtained for the two parameters in this paper. This can be explained if it is assumed that reaction kinetics are rate-controlling at low pressures and flame spreading is controlling at higher pressures, as follows: Consider figure 19, which shows operating curves for three hypothetical combustors 7, 8, and 9. Combustor 7 gives substantially 100-percent combustion efficiency throughout the high-pressure range where flame spreading controls the combustion rate; its efficiency drops below 100 percent only at the low pressures where reaction kinetics control the over-all rate of combustion. Hence, the data for this combustor would be expected to correlate with the reaction-kinetics parameter $P_t T_t/V_r$ or P_t^2/w_a. Combustor 9, on the other hand, will not operate at low pressures, and its performance should therefore correlate with the flame-spreading parameter $P_t^{0.24} T_t/V_r^{0.76}$, which is equivalent to $P_t^{1.0} T_t^{0.24}/w_a^{0.76}$, or $P_t^{1.32}/w_a$ for tests where T_t is constant. Combustor 8 gives low efficiencies at pressure levels where both flame spreading and reaction kinetics are controlling. Its performance data cannot be correlated with either of the preceding parameters by itself. For a perfect correlation the kinetics parameter should be used for the lower operating pressures and the flame-spreading parameter for the higher pressures. If all the data are plotted against a single parameter, however, then the best correlation should be obtained with some parameter P_t^n/w_a, where $1.32<n<2$. Thus, this argument can account for the fact that each investigator (e. g., refs. 26 and 27) seems to obtain a different correlating parameter for the particular combustor investigated.

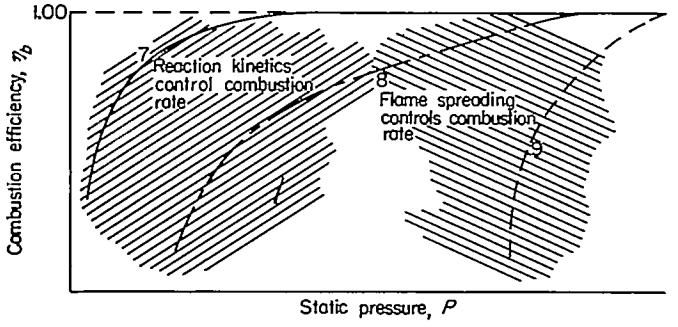

FIGURE 19.—Performance curves for three hypothetical combustors. For combustor 7, P_t^2/w_a should correlate η data. For combustor 9, $P_t^{0.24}/w_a^{0.76}$ should correlate η data. For combustor 8, P_t^n/w_a, where $1.3<n<2$, should provide best correlation of η data obtainable with a single parameter; however, no single parameter is really adequate for this combustor.

The hypothesis that reaction kinetics are rate-controlling at low pressures and flame spreading is controlling at higher pressures also gives some insight into the reasons why the reaction-kinetics parameter better correlates most turbojet combustor data while the flame-spreading parameter is better for the small-scale ramjets of figure 7. These ramjets could not operate at combustor pressures below 15 inches of mercury, while many of the turbojet combustors have been operated to much lower pressures. The story is not quite this straightforward, however, for in some turbojet combustors which gave low efficiencies at pressures above 15 inches of mercury the reaction-kinetics parameter has given better data correlations than the flame-spreading parameter. Perhaps the pressure level at which the transition occurs from one rate-controlling process to the other is appreciably different in different combustors.

CONCLUDING REMARKS

The parameter $P_t T_t/V_r$, which was derived from the assumption that chemical reaction kinetics control combustor performance, provides an adequate correlation of the combustion-efficiency data of most turbojet combustors at simulated engine operating conditions. Many of these same data are not correlated by the parameter $P_t^{0.24} T_t/V_r^{0.76}$, derived from the assumption that the rate of flame spreading controls combustor performance. The flame-spreading parameter does, however, correlate data obtained with two small

ramjet combustors. Data obtained with one turbojet combustor indicated that a shift from one rate-controlling step to another occurs as combustor pressure is increased, and the parameter $P_t T_t / V_r$ therefore best correlates the data at low pressures while the parameter $P_t^{0.24} T_t / V_r^{0.76}$ is better at higher pressures. No single correlating parameter can therefore be expected to be adequate for all combustors and for the entire range of operating conditions.

Combustor performance data are not available for wide ranges of inlet-air temperature. The maximum variation in T_t was 50 percent for the test data used to evaluate the correlating parameter. Consequently, some doubt exists whether the parameters derived herein would be adequate if larger T_t variations were encountered.

Because of the complexity of the over-all process of turbine-engine combustion, it appears unlikely that this simplified theoretical treatment (which assumes one step in the conversion processes to be rate-controlling) would be adequate for all combustors. Previous investigations have shown that the parameter $P_t T_t / V_r$ is not adequate for correlating the data for certain turbojet combustors, even for the limited range of conditions required to simulate flight operation. In addition, experimental data are available that indicate fuel vaporization and fuel-air mixing play an important role in some combustors (unpublished NACA data). Consequently, the equations derived in this paper must be applied judiciously and with due regard for their limitation.

The practical use of the parameter $P_t T_t / V_r$ for predicting the performance of new combustor designs is discussed in reference 28.

LEWIS FLIGHT PROPULSION LABORATORY
NATIONAL ADVISORY COMMITTEE FOR AERONAUTICS
CLEVELAND, OHIO, *August 5, 1957*

APPENDIX A

SYMBOLS

A_a	average cross-sectional area of combustor reaction zone, sq ft
A_h	liner air-entry hole area, sq ft
$\sum_p A_h$	hole area in primary zone, sq ft
$\sum_t A_h$	total hole area in liner, sq ft
A_r	maximum cross-sectional area of combustor flow passage, sq ft
C_d	discharge coefficient of liner holes
E	energy of activation for reaction, ft-lb/lb
$K_1, K_2,$ $K_3, \ldots$	constants
L	length of reaction zone, ft
l	distance from upstream end of reaction zone to plane of any point within reaction zone, ft
N_A, N_B	number of molecules of reactants A and B per pound of original mixture, lb^{-1}
P	static pressure in combustor reaction zone, lb/sq ft abs
P_t	combustor-inlet static pressure, lb/sq ft abs
ΔP	static-pressure drop across combustor, lb/sq ft abs
R	gas constant, ft-lb/(lb)(°R)
Re	Reynolds number
S	total flame surface area in combustor, sq ft
T	absolute static temperature in combustor reaction zone, °R
T_{eq}	equilibrium flame temperature, °R
T_t	combustor-inlet absolute static temperature, °R
ΔT_s	temperature rise for complete combustion of stoichiometric mixture, °F
t	time, sec
U_L	laminar flame speed, ft/sec
U_T	turbulent flame speed, ft/sec
V_{av}	velocity based on density, mass flow, and average cross-sectional area of reaction zone, ft/sec
V_r	reference velocity based on combustor-inlet density, total airflow, and maximum cross-sectional area of combustor flow passage, ft/sec
W	weight of mixture reacted at any time t, lb/cu ft
dW/dt	reaction rate, lb mixture reacting/(sec)(cu ft)
w_a	combustor airflow rate, lb/sec
X	fraction of N reacted at any time t or at any location within reaction zone
Z	number of molecular collisions of type involved in reaction, per unit time, $ft^{-3}sec^{-1}$
α	volume-percent oxygen concentration at combustor inlet
β	probability factor, fraction of collisions involving sufficient energy for reaction to occur which actually result in reaction
η_b	combustion efficiency
ρ	density, lb/cu ft
ρ_u	density of unburned gas, lb/cu ft
σ_A, σ_B	effective molecular diameter of reactants A and B, ft
φ	fraction of collisions involving sufficient energy for reaction to occur

APPENDIX B

SIMPLIFIED DERIVATION OF KINETICS EQUATIONS

For the bimolecular reaction, A+B→C+D, in which A is the reactant present in smaller quantity, the reaction rate is given by the equation

$$\frac{dW}{dt}=\frac{Z\varphi\beta}{N_A} \tag{1}$$

The probability factor β will be assumed to be constant, which is conventional.

A molecular collision of the required type (A+B) occurs when the distance between the centers of the molecules is $(\sigma_A+\sigma_B)/2$. The average A molecule will therefore sweep out in unit time a cylindrical space of length u having an effective cross section of $(\pi/4)(\sigma_A+\sigma_B)^2$. The number of collisions of the average A molecule with B molecules per unit time will be $(\pi/4)(\sigma_A+\sigma_B)^2 u n_B$. Each of the other A molecules is also colliding with B molecules; the total number of A+B collisions per unit time per unit volume is therefore

$$Z=\frac{\pi}{4}(\sigma_A+\sigma_B)^2 u n_A n_B$$

Certain approximations are involved in this derivation; and, when corrections are made for the distribution of molecular velocities and other factors, the equation becomes

$$Z=K_1(\sigma_A+\sigma_B)^2 u n_A n_B \tag{B1}$$

Substituting $\sqrt{K_7 RT}$ for u, $\rho N_A(1-X)$ for n_A, and $\rho N_B\left(1-\frac{N_A}{N_B}X\right)$ for n_B gives

$$Z=K_3(\sigma_A+\sigma_B)^2(RT)^{1/2}(N_A N_B)(1-X)\left(1-\frac{N_A}{N_B}X\right)\rho^2$$

When P/RT is substituted for ρ,

$$Z=\frac{K_3(\sigma_A+\sigma_B)^2 N_A N_B(1-X)\left(1-\frac{N_A}{N_B}X\right)P^2}{R^{3/2}T^{3/2}} \tag{B2}$$

From the Maxwell-Boltzmann distribution law (ref. 9),

$$\varphi=e^{-E/RT} \tag{B3}$$

Equations (B3) and (B4) are substituted in (1) to obtain

$$\frac{dW}{dt}=\frac{K_3(\sigma_A+\sigma_B)^2 N_B(1-X)\left(1-\frac{N_A}{N_B}X\right)P^2 e^{-E/RT}}{R^{3/2}T^{3/2}} \tag{B4}$$

Now

$$\frac{dX}{dt}=\frac{1}{\rho}\frac{dW}{dt}=\frac{K_3(\sigma_A+\sigma_B)^2 N_B(1-X)\left(1-\frac{N_A}{N_B}X\right)P e^{-E/RT}}{R^{1/2}T^{3/2}} \tag{2}$$

APPENDIX C

KINETICS EQUATION EXPRESSED IN TERMS OF MEASURED QUANTITIES

Equations (2) and (4) are expressed in terms of quantities P, T, and V_a, in the combustion zone. In most experimental investigations these quantities are not measured. It is therefore desirable to express these equations in terms of the measured quantities P_t, T_t, and V_r. This can be done as follows:

$$P=P_t\left(1-\frac{\Delta P}{P_t}\right) \tag{C1}$$

where $\Delta P/P_t \approx 0.05$ for most turbojet combustors;

$$V_a=\left(\frac{V_r}{1-\frac{\Delta P}{P_t}}\right)\left(\frac{T}{T_t}\right)\left(\frac{A_r}{A_a}\right)\left(\frac{\sum_p A_h C_d}{\sum_t A_h C_d}\right) \tag{C2}$$

where $A_r/A_a \approx 1.7$ for most turbojet combustors. Substituting these expressions into equation (4) gives

$$\ln\frac{1-\frac{N_A}{N_B}\eta_b}{1-\eta_b}+K_2$$

$$=\frac{K_3(\sigma_A+\sigma_B)^2(N_B-N_A)e^{-E/RT}}{R^{1/2}T^{3/2}}\left[\frac{L\left(1-\frac{\Delta P}{P_t}\right)^2}{\frac{\sum_p A_h C_d}{\sum_t A_h C_d}\left(\frac{A_r}{A_a}\right)}\right]\frac{P_t T_t}{V_r} \tag{5}$$

REFERENCES

1. Childs, J. Howard, McCafferty, Richard J., and Surine, Oakley W.: Effect of Combustor-Inlet Conditions on Performance of an Annular Turbojet Combustor. NACA Rep. 881, 1947. (Supersedes NACA TN 1357.)
2. Childs, J. Howard: Preliminary Correlation of Efficiency of Aircraft Gas-Turbine Combustors for Different Operating Conditions. NACA RM E50F15, 1950.
3. Graves, Charles C.: Effect of Oxygen Concentration of the Inlet Oxygen-Nitrogen Mixture on the Combustion Efficiency of a Single J33 Turbojet Combustor. NACA RM E52F13, 1952.
4. Graves, Charles C.: Effect of Inlet Oxygen Concentration on Combustion Efficiency of J33 Single Combustor Operating with Gaseous Propane. NACA RM E53A27, 1953.
5. Childs, J. Howard, and Graves, Charles C.: Relation of Turbine-Engine Combustion Efficiency to Second-Order Reaction Kinetics and Fundamental Flame Speed. NACA RM E54G23, 1954.
6. Reynolds, Thaine W., and Ingebo, Robert D.: Combustion Efficiency of Homogeneous Fuel-Air Mixtures in a 5-Inch Ram-Jet-Type Combustor. NACA RM E52I23, 1952.
7. Reynolds, Thaine W.: Effect of Fuels on Combustion Efficiency of 5-Inch Ram-Jet-Type Combustor. NACA RM E53C20, 1953.
8. Childs, J. Howard, and Graves, Charles C.: Correlation of Turbine-Engine Combustion Efficiency with Theoretic Equations. Sixth Symposium (International) on Combustion, Reinhold Pub. Corp., 1957, pp. 869–878.
9. Kassel, Louis S.: The Kinetics of Homogeneous Gas Reactions. Chem. Catalog Co. (N. Y.), 1932.
10. Avery, W. H., and Hart, R. W.: Combustor Performance with Instantaneous Mixing. Ind. and Eng. Chem., vol. 45, no. 8, Aug. 1953, pp. 1634–1637.
11. Longwell, John P., Frost, Edward E., and Weiss, Malcom A.: Flame Stability in Bluff Body Recirculation Zones. Ind. and Eng. Chem., vol. 45, no. 8, Aug. 1953, pp. 1629–1633.
12. Bollinger, Lowell M., and Williams, David T.: Effect of Reynolds Number in the Turbulent-Flow Range on Flame Speed of Bunsen-Burner Flames. NACA Rep. 932, 1949. (Supersedes NACA TN 1707.)
13. Fine, Burton D.: Effect of Pressure on Turbulent Burning Velocity. (To be published in Combustion and Flame.)
14. Wagner, Paul: Burning Velocities of Various Premixed Turbulent Propane Flames on Open Burners. NACA TN 3575, 1955.
15. Dugger, Gordon L., and Graab, Dorothy D.: Flame Speeds of 2,2,4-Trimethylpentane-Oxygen-Nitrogen Mixtures. NACA TN 2680, 1952.
16. Gaydon, A. G., and Wolfhard, H. G.: The Influence of Diffusion on Flame Propagation. Proc. Roy. Soc. (London), ser. A, vol. 196, 1949, pp. 105–113.
17. Garner, F. H., Ashforth, G. K., and Long, R.: The Effect of Pressure on Burning Velocities of Benzene-Air, *n*-Heptane-Air and 2,2,4-Trimethylpentane-Air Mixtures. Fuel, vol. XXX, no. 1, Jan. 1951, pp. 17–19.
18. Penner, S. S.: Spectroscopic Studies of Premixed Laminar Flames. Selected Combustion Problems, Fundamentals and Aero. Applications, Butterworths Sci. Pub. (London), 1954, pp. 144–166; discussion, pp. 167–191.
19. Singer, J. M., Grumer, Joseph, and Cook, E. B.: Burning Velocities by the Bunsen-Burner Method. I—Hydrocarbon-Oxygen Mixtures at One Atmosphere. II—Hydrocarbon-Air Mixtures at Subatmospheric Pressures. Proc. Gas Dynamics Symposium on Aerothermochemistry, Northwestern Univ., Aug. 22–23–24, 1955, pp. 139–150.
20. Cullen, R. E.: A Non-Dimensional Correlation of Flame Propagation at Subatmospheric Pressures. Trans. ASME, vol. 75, no. 1, Jan. 1953, pp. 43–49.
21. Graves, C. C.: Combustion of Single Isooctane Drops in Various Quiescent Oxygen-Nitrogen Atmospheres. Proc. Third Midwestern Conf. on Fluid Mech., Univ. Minn., 1953, pp. 759–778.
22. Lewis, Bernard, and von Elbe, Guenther: Combustion, Flames and Explosions of Gases. Academic Press, Inc., 1951.
23. Hottel, H. C., Williams, G. C., and Satterfield, C. N.: Thermodynamic Charts for Combustion Processes, pts. I and II. John Wiley & Sons, Inc., 1949.
24. Jost, Wilhelm: Explosion and Combustion Processes in Gases. McGraw-Hill Book Co., Inc., 1946, p. 476.
25. Coward, H. F., and Jones, G. W.: Limits of Flammability of Gases and Vapors. Bull. 503, Bur. Mines, 1952.
26. Greenhough, V. W., and Lefebvre, A. H.: Some Applications of Combustion Theory to Gas Turbine Development. Sixth Symposium (International) on Combustion, Reinhold Pub. Corp., 1957, pp. 858–869.
27. Woodward, E. C.: Similitude Study of Idealized Combustors. Sixth Symposium (International) on Combustion, Reinhold Pub. Corp., 1957, pp. 849–858.
28. Olson, Walter T., Childs, J. Howard, and Scull, Wilfred E.: Method for Estimating Combustion Efficiency at Altitude Flight Conditions from Combustor Tests at Low Pressures. NACA RM E53F17, 1953.